Estuaries and Coasts
DOI 10.1007/s12237-013-9656-6

Scientific Bases for Numerical Chlorophyll Criteria in Chesapeake Bay

L. W. Harding Jr. · R. A. Batiuk · T. R. Fisher · C. L. Gallegos · T. C. Malone · W. D. Miller · M. R. Mulholland · H. W. Paerl · E. S. Perry · P. Tango

Received: 17 September 2012 / Revised: 30 May 2013 / Accepted: 31 May 2013

Abstract In coastal ecosystems with long flushing times (weeks to months) relative to phytoplankton growth rates (hours to days), chlorophyll *a* (*chl-a*) integrates nutrient loading, making it a pivotal indicator with broad implications for ecosystem function and water-quality management. However, numerical *chl-a* criteria that capture the linkage between *chl-a* and ecosystem impairments associated with eutrophication (e.g., hypoxia, water clarity and loss of submerged aquatic vegetation, toxic algal blooms) have seldom been developed despite the vulnerability of these ecosystems to anthropogenic nutrient loading. Increases in fertilizer use, animal wastes, and population growth in the Chesapeake Bay watershed since World War II have led to increases in nutrient loading and *chl-a*. We describe the development of numerical *chl-a* criteria based on long-term research and monitoring of the bay. Baseline *chl-a* concentrations were derived using statistical models for historical data from the 1960s and 1970s, including terms to account for the effects of climate variability. This approach produced numerical *chl-a* criteria presented as geometric means and 90th percentile thresholds to be used as goals and compliance limits, respectively. We present scientific bases for these criteria that consider specific ecosystem impairments linked to increased *chl-a*, including low dissolved oxygen (DO), reduced water clarity, and toxic algal blooms. These multiple lines of evidence support numerical *chl-a* criteria consisting of seasonal mean *chl-a* across salinity zones ranging from 1.4 to 15 mg m^{-3} as restoration goals and corresponding thresholds ranging from 4.3 to 45 mg m^{-3} as compliance limits. Attainment of these goals and limits for *chl-a* is a precondition for attaining desired levels of DO, water clarity, and toxic phytoplankton prior to rapid human expansion in the watershed and associated increases of nutrient loading.

Electronic supplementary material The online version of this article (doi:10.1007/s12237-013-9656-6) contains supplementary material, which is available to authorized users.

L. W. Harding Jr. · T. R. Fisher · T. C. Malone
Horn Point Laboratory, University of Maryland Center for Environmental Science, 2020 Horns Point Road, Box 775, Cambridge, MD 21613, USA

L. W. Harding Jr. (✉)
Department of Atmospheric and Oceanic Sciences, University of California, Los Angeles, Los Angeles, CA 90095, USA
e-mail: lharding@atmos.ucla.edu

R. A. Batiuk
Chesapeake Bay Program Office, U.S. Environmental Protection Agency, 410 Severn Avenue, Annapolis, MD 21403, USA

C. L. Gallegos
Smithsonian Environmental Research Center, PO Box 28, Edgewater, MD 21037, USA

W. D. Miller
U.S. Naval Research Laboratory, 4555 Overlook Ave., SW, Washington, DC 20375, USA

M. R. Mulholland
Department of Ocean, Earth and Atmospheric Science, Old Dominion University, 4600 Elkhorn Ave., Norfolk, VA 23529, USA

H. W. Paerl
Institute of Marine Sciences, University of North Carolina at Chapel Hill, 3431 Arendell Street, Morehead City, NC 28557, USA

E. S. Perry
2000 Kings Landing Road, Huntingtown, MD 20639, USA

P. Tango
Maryland Department of Natural Resources, 580 Taylor Avenue, Annapolis, MD 21401, USA

Published online: 18 June 2013

Keywords Phytoplankton · Chlorophyll · Water quality criteria · Estuaries · Chesapeake Bay

Introduction

As an index of phytoplankton biomass, chlorophyll *a* concentration (*chl-a*) is an important measure of water quality in estuaries such as Chesapeake Bay. Significant seasonal and interannual increases of *chl-a* since World War II have been related to increases in anthropogenic nutrient loading to the estuary (cf. Harding and Perry 1997). Contemporary loadings of total nitrogen (TN) and total phosphorus to the bay and its tributaries have reached ~14 g N m^{-2}-$year^{-1}$ and 1.1 g P m^{-2} $year^{-1}$, respectively (Boynton et al. 1995), including a 2.5-fold increase of TN loading from the Susquehanna River between 1945 and 2001 that has decreased slightly thereafter (Hagy et al. 2004). Compelling scientific evidence has led to a consensus that anthropogenic loads of N and P underlie the degradation of water quality in this large (11,600 km^2) estuarine ecosystem (Kemp et al. 2005).

Climate variability significantly affects *chl-a* in the bay via freshwater runoff and associated delivery of sediments and nutrients from an extensive (165,000 km^2) watershed (Malone 1992; Harding and Perry 1997; Adolf et al. 2006; Miller and Harding 2007). Long-term discharge records for the Susquehanna River (US Geological Survey—http://waterdata.usgs.gov) and a synoptic climatology for the mid-Atlantic region (Miller et al. 2006) reveal wet and dry years. Since the mid-1980s, this pattern has been associated with large seasonal and interannual variations in *chl-a* and associated impairments (Malone et al. 1988, 1996; Miller and Harding 2007). Consequently, it has been difficult to resolve a secular trend of *chl-a* during this period (Harding and Perry 1997).

Efforts to develop *chl-a* criteria have resulted in subjective narrative criteria that are intended to promote "habitat health" in the bay:

> Concentrations of chlorophyll-*a* in free floating microscopic plants (algae) shall not exceed levels that result in ecologically undesirable consequences—such as reduced water clarity, low dissolved oxygen (DO), food supply imbalances, proliferation of species deemed potentially harmful to aquatic life or humans or aesthetically objectionable conditions—or otherwise render tidal waters unsuitable for designated uses (Chapter V, p. 103 in US Environmental Protection Agency 2003).

The absence of numerical *chl-a* criteria constituting objective, scientifically sound goals based on ecosystem impairments, however, limits the evaluation of progress toward restoration.

Research and monitoring over the last half century have identified specific ecosystem impairments associated with nutrient over-enrichment and high *chl-a* in Chesapeake Bay. These include seasonal hypoxia and anoxia (Malone 1992; Smith et al. 1992; Hagy et al. 2004; Bricker et al. 2007), decreased water clarity and associated declines in the spatial extent of submerged aquatic vegetation (SAV) (Dennison et al. 1993; Kemp et al. 2004), and toxic algal blooms (Marshall et al. 2005, 2009; Mulholland et al. 2009; Morse et al. 2011). Here we present scientific bases to establish numerical *chl-a* criteria that will aid decision makers in restoring and sustaining the water quality of coastal ecosystems.

We posed the following questions:

- How can quantitative links between *chl-a* and specific ecosystem impairments be established?
- How well do numerical (quantitative) *chl-a* criteria based on these different ecosystem impairments agree?

Three approaches were used to address these questions: (1) establish baseline *chl-a* by analyzing historical and recent data with statistical models, (2) quantify effects of climate variability on *chl-a* by including terms for freshwater flow in the models, and (3) identify relationships between *chl-a* and specific ecosystem impairments. Results are consistent suggesting a way forward for other coastal ecosystems where flushing times are long relative to phytoplankton generation times.

Methods

Historical *chl-a*

Measurements of *chl-a* are not available for Chesapeake Bay prior to the onset of anthropogenic influence. However, extensive data from research and monitoring spanning six decades provide time series of measurements that provide useful reference points to establish numerical *chl-a* criteria. We used historical data (1950–1983) from archives of the Environmental Protection Agency Chesapeake Bay Program (CBP) and monitoring data from the Chesapeake Bay Water Quality Monitoring Program (hereafter CBP Monitoring Program, 1985–2011) to determine baseline *chl-a*. Spatial and temporal coverage of *chl-a* in the 1950s was too limited to derive numerical *chl-a* criteria, but data for the 1960s and 1970s were sufficiently resolved to support our analyses. We reasoned that numerical *chl-a* criteria reflecting earlier conditions might be attainable by achieving nutrient reductions, despite the fact that *chl-a* in the 1960s and 1970s did not represent conditions for an unimpaired ecosystem.

An earlier analysis (Harding and Perry 1997) was extended using surface *chl-a* and vertical *chl-a* profiles for 1950 through

2011 from the CBP data hub (http://www.chesapeakebay.net). Analytical methods, including filter type, solvent, instrumentation, equations, and calibration, were evaluated and geo-referenced data were assembled from sources that used comparable methods as described by Harding and Perry (1997). Depth-averaged water column *chl-a* was computed from vertical profiles. Data were aggregated for oligohaline (OH), mesohaline (MH), and polyhaline (PH) salinity zones (Fig. 1) to capture along-axis variability of key water-quality properties that affect the spatial distribution of *chl-a* (Harding et al. 1986; Fisher et al. 1988). Seasonal aggregations consisted of five categories defined as winter (January, February, March), spring (April, May), transition (June), summer (July, August, September), and fall (October, November, December) to capture the annual phytoplankton cycle in the bay (Malone 1992; Harding and Perry 1997).

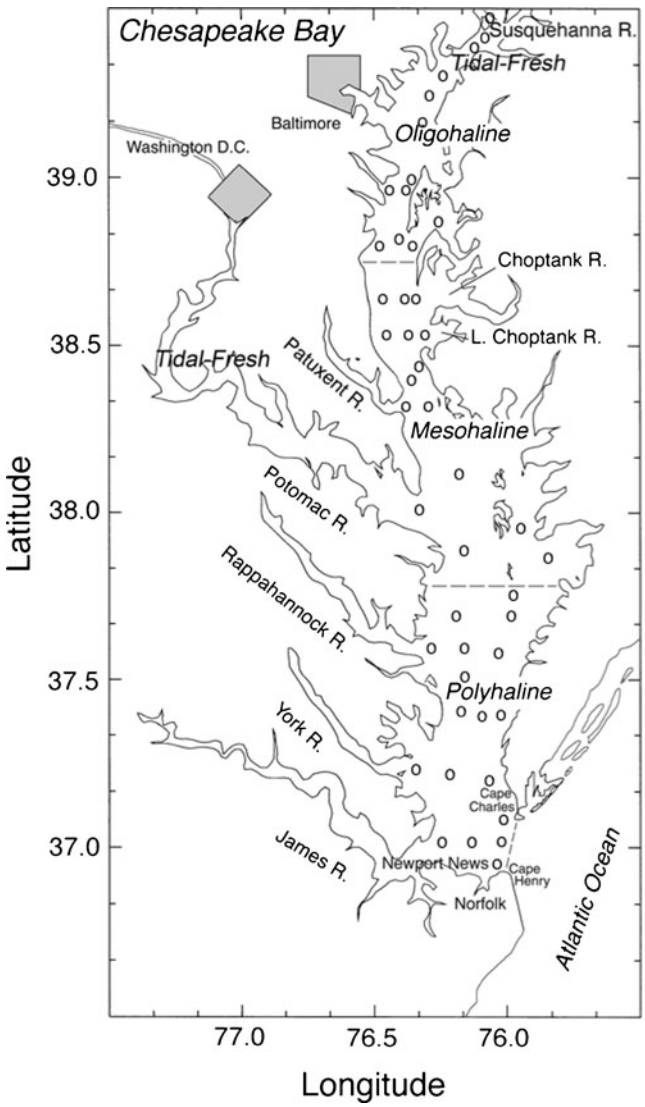

Fig. 1 Map of Chesapeake Bay showing major cities, tributaries, salinity zones, and station locations

Surface and depth-averaged *chl-a* were logarithmically transformed (base 10) to achieve normality and used as dependent variables in generalized additive models (GAMs) and general linear models (GLMs) (Wood 2006; SAS Institute, Inc 1993). GAMs were used to quantify historical trends of flow-adjusted annual mean *chl-a.* GLMs were used to determine characteristic distributions of *chl-a* by decade, season, and salinity zone while segregating effects due to climate-driven variability of freshwater flow. A set of eight variables was selected, consisting of decade, month (within season), season, salinity zone, two-way interactions of decade and salinity zone, decade and season, decade and month, and salinity zone and season, and a three-way interaction of decade, salinity zone, and season.

Observations for wet and dry years corresponding to high-flow and low-flow conditions, respectively, were used to develop numerical *chl-a* criteria to account for climate variability. We used salinity nested within a salinity zone as an independent variable in GLMs to capture the effects of freshwater flow. Nesting salinity as a continuous variable within a categorical salinity zone assured the salinity term represented flow rather than the spatial distribution of *chl-a* along the salinity gradient of the bay. Historical data were compiled from projects with distinct goals and sampling designs, resulting in unequal temporal coverage, and we were unable to estimate flow-lag and flow-averaging windows to use freshwater flow directly as an independent variable in GLMs. A direct correspondence between salinity and freshwater flow was confirmed using data from the CBP Monitoring Program and US Geological Survey. For each month and decade, the 10th percentile, median, and 90th percentile of salinity were computed for each salinity zone. A synthetic prediction data set with $\log_{10}$ *chl-a* set to "missing" was created with one observation for each decade, month, salinity zone, and salinity value. Water temperature and station depth were set to median values. The predicted value of $\log_{10}$ *chl-a* was obtained using a GLM for each of these synthetic observations. Outputs were: GLM (10th salinity percentile)=high-flow prediction; GLM (median salinity percentile)=mid-flow prediction; GLM (90th salinity percentile)=low-flow prediction.

Climate conditions were categorized as wet, long-term average (LTA), or dry using daily freshwater flow from the Susquehanna River (US Geological Survey) and a synoptic climatology for the mid-Atlantic region based on sea-level pressure patterns (Miller et al. 2006). Flow-based categorizations used the long-term (1945–2011) annual mean discharge of 35.5×10^9 m^3 year^{-1} as a cutoff point. Values 10 % greater than the mean were considered wet and those 10 % less than the mean were considered dry. Synoptic climatology categorizations used frequencies of ten sea-level pressure patterns capturing regional weather with data from the National Climate Data Center. Climate conditions (wet precipitation) indicated by freshwater flow and synoptic

climatology were compared, and each year was assigned a designation to aggregate *chl-a* data.

Geometric means (GMs) and 90th percentile thresholds of surface and depth-averaged *chl-a* were determined for each historical reference period, salinity zone, and climate condition. Mean *chl-a* was defined as the "goal" based on a historical reference period, and the corresponding 90th percentile threshold *chl-a* was the "compliance limit" above the mean that should rarely be exceeded by a population of *chl-a* characterizing that period. The upper threshold was based on the distribution of values for a uni-dimensional population of *chl-a* for the 1960s and 1970s using the 90th percentile to allow 10 % non-compliance. Selection of 10 % as an allowable frequency of non-compliance was based on guidance from environmental managers and the availability of extensive data from the CBP Monitoring Program to test compliance (US Environmental Protection Agency 2003). Additional details on statistical methods are presented in Supplemental Material.

Dissolved Oxygen

Numerical *chl-a* criteria were derived from relationships between *chl-a* and DO using 20 years of data from the CBP Monitoring Program (1985–2004). DO, *chl-a*, salinity, and temperature data were acquired for 15 stations in oligohaline, mesohaline, and polyhaline salinity zones in mainstem Chesapeake Bay and one station near the mouths of two tidal tributaries (Choptank and Patuxent Rivers) using the CBP data hub (Fig. 1). Several models of Yellow Springs Instruments and Sea-Bird sensors were used to measure DO, salinity, and temperature on cruises conducted one to two times per month. A Turner Designs model 10 fluorometer calibrated with pure *chl-a* standards was used to determine *chl-a* on acetone extracts of particulates collected on Whatman GF/F filters. Data were aggregated over several time frames, including calendar year, water year, and season, to capture the seasonal offset of *chl-a* maxima and DO minima in establishing relationships.

Statistical relationships were analyzed using SigmaPlot v.11 integrated with SigmaStat v.3. Simple linear and multiple linear regression (MLR) models were applied to mean summer bottom-water DO and water depth, surface *chl-a*, and the salinity difference between surface and bottom waters (ΔS) to develop relationships for the bay and tributaries. The Choptank River represented a rural tributary on the eastern shore of the bay with low population density (59 km^{-2}) and significant agriculture (61 % of land use), and the Patuxent River represented a more developed tributary on the western shore with high population density (262 km^{-2}) and high wastewater inputs (235×10^6 L day^{-1}) (Fisher et al. 2006).

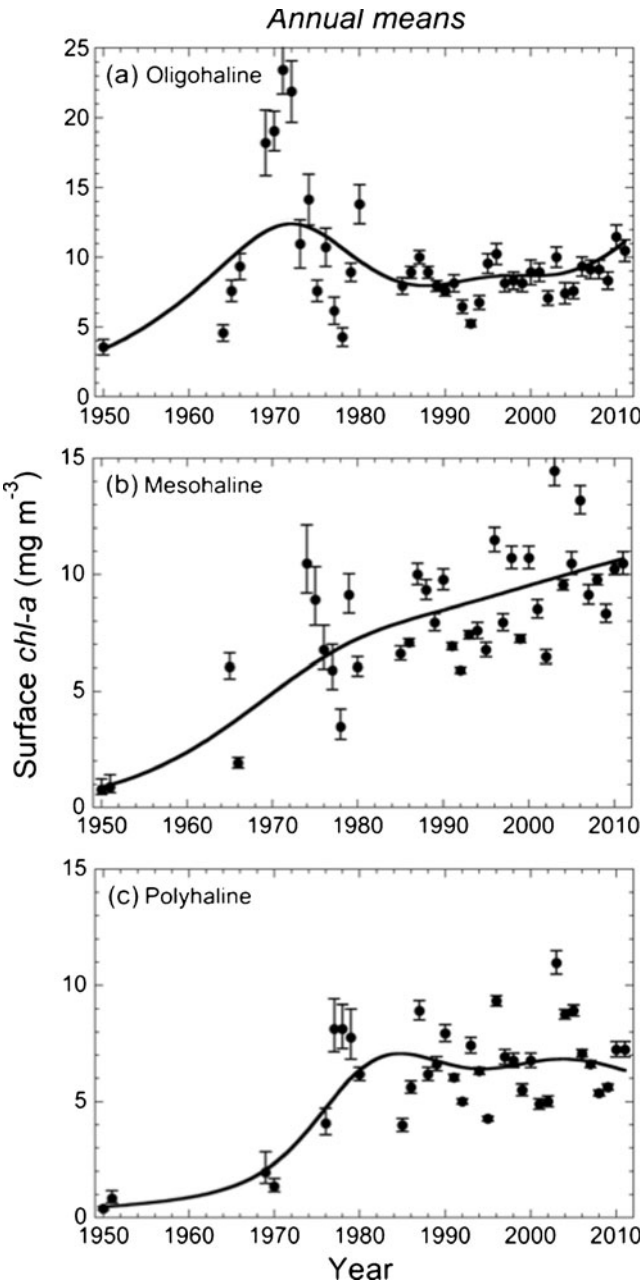

Fig. 2 a–c Time-series (1950–2011) of annual geometric means (GM±SE) of surface *chl-a* for three salinity zones in Chesapeake Bay. Curves are outputs of GAMs that were highly significant ($p<0.001$)

Water Clarity

Numerical *chl-a* criteria were derived based on the light requirements of SAV to meet restoration targets for Chesapeake Bay (Batiuk et al. 1992). This approach recognizes that light penetration sufficient to support SAV places a constraint on *chl-a* (Gallegos 1994, 2001). Correspondence analysis between SAV distribution and light attenuation indicated that SAV in the oligohaline salinity zone require on average 13 %

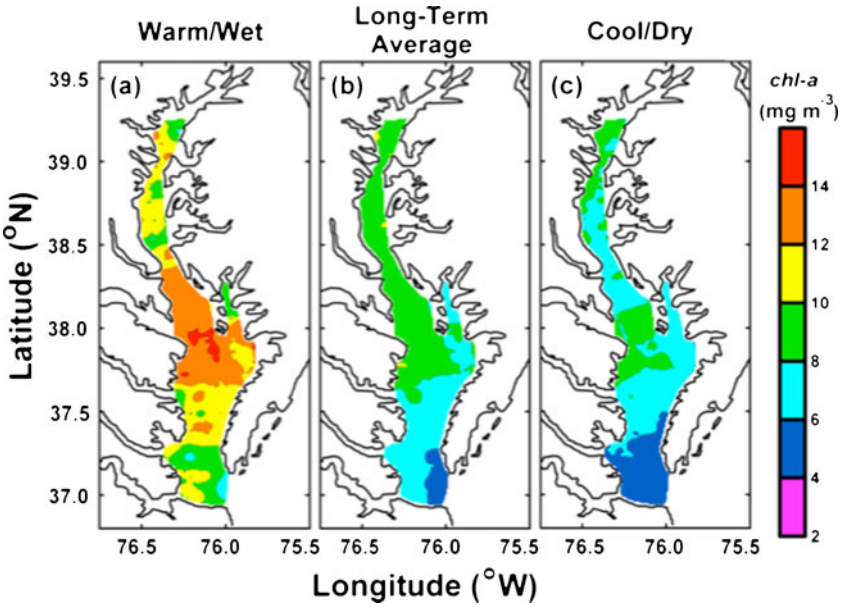

Fig. 3 **a**–**c** Surface *chl-a* during the spring bloom from airborne remote sensing of ocean color in Chesapeake Bay (http://www.cbrsp.org) in: **a** warm/wet; **b** long-term average; **c** cool/dry conditions (adapted from Miller and Harding 2007). These images depict average March to May *chl-a* using data interpolated at 1-km^2 resolution and aggregated by prevailing climate conditions

of surface irradiance, while those growing in mesohaline and polyhaline salinity zones require 22 % (Carter et al. 2000; Kemp et al. 2004). Radiative transfer modeling using *Hydrolight* 4.2 was used to link inherent optical properties (i.e., absorption and scattering coefficients) to the attenuation coefficient for downwelling irradiance, K_d (Kirk et al. 1994; Mobley 1994). Concentrations of *chl-a* and other bio-optically active constituents allowing penetration of specified percentages of PAR (13 or 22 %, depending on salinity zone) to depths historically known to support SAV were computed.

Light attenuation in the water column is associated with pure water and three classes of materials, including *chl-a*, colored dissolved organic matter (CDOM), and non-algal particulates (NAP) (Roesler et al. 1989). We derived *chl-a* criteria by allocating a fixed fraction of the allowable attenuation to *chl-a* beyond that due to pure water alone. We chose the fraction 0.30 (30 %) for attenuation by *chl-a* based on extensive bio-optical observations in lower Chesapeake Bay and the mid-Atlantic Bight (Magnuson et al. 2004; Schofield et al. 2004; Harding et al. 2005), a suitable reference condition that will prevent dominance of attenuation by *chl-a*. By this approach, *chl-a* is independent of other factors (CDOM, NAP) that may dominate light attenuation in other sections of the bay. Sensitivity of calculated *chl-a* criteria to the fraction of attenuation allocated to *chl-a* was also examined with the fraction set at 0.25 and 0.35.

Depths to which SAV once grew vary with location, and the concentrations of attenuators allowing adequate light penetration for SAV depend greatly on this depth. An analysis of historical SAV coverage in the bay was used to assign "application depths" of 0.5, 1.0, or 2.0 m based on the light

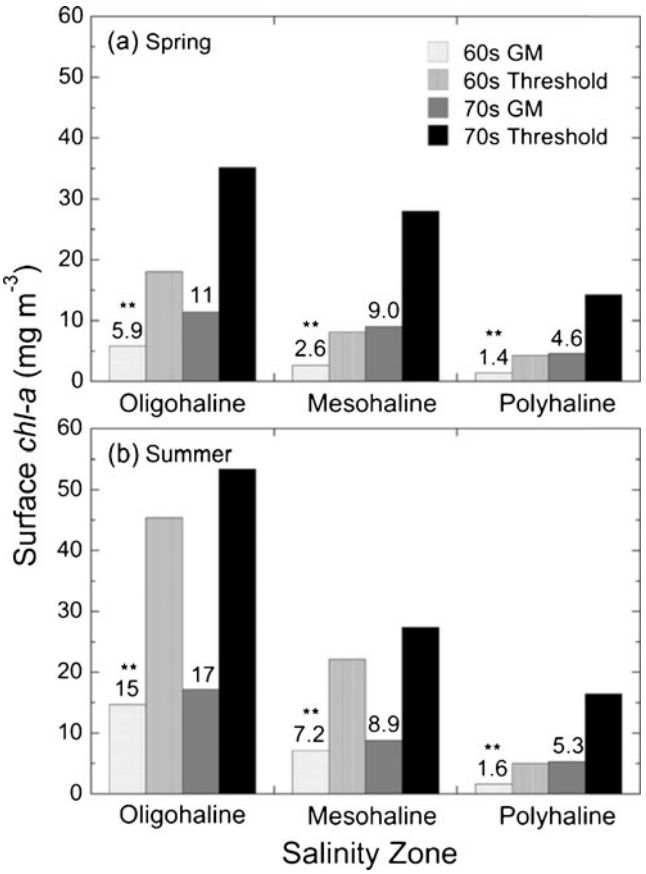

Fig. 4 **a**, **b** GMs and 90th percentile thresholds of surface *chl-a* under mid-flow conditions for 1960s and 1970s historical reference periods by salinity zone. *Asterisks over data bars* identify GMs for the 1960s to highlight surface *chl-a* values that we are presenting as goals

Table 1 Summary of numerical *chl-a* criteria based on the 1960s historical reference period including flow-adjusted values to account for climate variability

Method	Season[a]	Salinity zone	Numerical *chl-a* criteria	
			Mean (mg m^{-3})	Threshold[b] (mg m^{-3})
Low-flow	Spring	OH	6.4	20
		MH	2.2	6.9
		PH	1.1	3.3
	Summer	OH	17	53
		MH	6.3	20
		PH	1.3	3.9
Mid-flow	Spring	OH	5.9	18
		MH	2.6	8.2
		PH	1.4	4.3
	Summer	OH	15	45
		MH	7.2	22
		PH	1.6	5.0
High-flow	Spring	OH	5.3	16
		MH	3.3	10
		PH	2.0	6.2
	Summer	OH	13	40
		MH	8.7	27
		PH	2.1	6.4

OH oligohaline, *MH* mesohaline, *PH* polyhaline

[a] Spring—Mar–May; summer—Jul–Aug

[b] 90th percentile *chl-a* concentration

requirements of SAV species (US Environmental Protection Agency 2003; Kemp et al. 2004). Fractions of surface PAR penetrating to these application depths with pure water as the only attenuator, F_{Zw}, were calculated using *Hydrolight*. Denoting the fraction of surface light required by SAV as F_{lr}, the fraction that must be transmitted by all other constituents is given by $\left(\frac{F_{lr}}{F_{Zw}}\right)$. Treating the water column above potential SAV habitat as a transmittance filter, the required transmittance allocated to *chl-a* is $\left(\frac{F_{lr}}{F_{Zw}}\right)^{0.3}$ and that allocated to all other constituents is $\left(\frac{F_{lr}}{F_{Zw}}\right)^{0.7}$. The fraction, $F_{chl\text{-}a}$, of surface PAR remaining at an application depth after attenuation by *chl-a* (and associated CDOM) is given by Eq. 1 as:

$$F_{\text{chl-a}} = F_{Zw}\left(\frac{F_{lr}}{F_{Zw}}\right)^{0.3} \quad (1)$$

Hydrolight was used to calculate the concentration of *chl-a* that allowed the fraction of surface PAR, $F_{chl\text{-}a}$, to penetrate to specific application depths. Additional details of the bio-optical model and *Hydrolight* simulations are given in the Supplemental Material.

Toxic Algal Blooms

The relationship between *chl-a* and abundance of *Microcystis* spp., a toxic algal species that has been linked to health risks in tributaries of Chesapeake Bay, was examined using data from the CBP Monitoring Program (1984–2006). *Microcystis* spp. form summer blooms and produce microcystins, forms of hepatotoxins that affect aquatic life and humans. Source data consisted of *chl-a* concentrations, cell counts of *Microcystis* spp. from preserved samples, salinity, water temperature, nutrient concentrations, water transparency, DO, and organic

Table 2 Summary statistics for simple linear regressions of mean summer bottom-water DO (in milligrams per liter) on surface *chl-a* (in milligrams per cubic meter) averaged over the designated intervals

Site	Regression statistic	Calendar year	Water year	Mean Jan–Aug *chl-a*	Mean May–Aug *chl-a*
Chesapeake Bay	R^2	0.23**	0.23**	0.23**	0.27**
	Slope	−0.123±0.020	−0.127±0.021	−0.098±0.016	−0.076±0.011
Tidal tributaries	R^2	0.12**	0.11**	0.11**	0.07*
	Slope	−0.105±0.025	−0.082±0.021	−0.076±0.020	−0.046±0.015

*$p<0.05$; **$p<0.01$ (significance levels)

carbon. Toxin concentrations were separately determined on live samples collected by the Maryland Department of Natural Resources (MD DNR, 2000–2006). Ecosystem impairments by toxic algal blooms were based on human-health risk, using published *chl-a* and microcystin concentrations that were converted from cell counts using a toxin yield per cell of 2×10^{-7} mg microcystin cell^{-1} (NHMRC 2005).

Classification and Regression Tree (CART) analysis, a non-parametric statistical method in S-Plus (2005) with no assumptions about linearity or normality of independent and dependent variables, was used to evaluate water quality relationships in the salinity range of 0–5 favorable to *Microcystis* spp. The response variable was abundance of *Microcystis* spp. as cell counts (in cells per liter) with three categories of human-health risk, and the independent variables were *chl-a*, phaeophytin, salinity, Secchi depth, orthophosphate (PO_4), dissolved inorganic nitrogen (NH_4, NO_2, NO_3), dissolved organic carbon, particulate carbon, and water temperature. Risk categories were based on cell counts obtained from the literature, where low-level risk was $<1\times10^7$ cells L^{-1}, mid-level risk was 1–5×10^7 cells L^{-1}, and high-level risk was $>5\times10^7$ cells L^{-1} (US Environmental Protection Agency 2007b). Low-level risk corresponded to protection from microcystin toxin levels >1 μg L^{-1} considered by the World Health Organization as a safety threshold for chronic drinking water exposure (Chorus and J. Bartram 1999; NHMRC 2005). Mid-level risk was considered protective of children, with minimal risk of exposure to microcystin >10 μg L^{-1} (NHMRC 2005). High-level risk corresponded to microcystin concentrations >10 μg L^{-1}. The *chl-a* thresholds derived from the CART analysis were compared with data from the CBP Monitoring Program for waters experiencing blooms of *Microcystis* spp. The frequency distribution of $\log_{10}$ *chl-a* was then used to compute mean $\log_{10}$ *chl-a* corresponding to the branch point from CART that represented the 90th percentile of the distribution.

Results

Historical *chl-a*

Phytoplankton biomass in Chesapeake Bay has increased during the past 60 years as shown by annual GMs of surface *chl-a* for 1950–2011 (Fig. 2a–c). GMs for the oligohaline salinity zone were ~3.5 mg m^{-3} in the early 1950s, increased to 4.5–9.3 mg m^{-3} in the 1960s, and reached 18–23 mg m^{-3} by the early 1970s. From the mid-1970s to 1985–2011, annual GMs declined from maxima >20 mg m^{-3} to current (2006–11) values of 9.1–11 mg m^{-3}. Annual GMs for the mesohaline salinity zone increased from 0.78–0.89 mg m^{-3} in 1950–51 to 1.9–6.0 mg m^{-3} by the mid-1960s, reaching 3.5–10 mg m^{-3} in the mid- to late-1970s. This upward trajectory was similar to that for the oligohaline salinity zone, except annual GMs for the mesohaline salinity zone continued to increase during the CBP Monitoring Program, reaching current (2006–11) values of 8.3–13 mg m^{-3}. Annual GMs for the polyhaline salinity zone increased from 0.39–0.83 mg m^{-3} in 1950–51 to 1.4–2.0 mg m^{-3} by the late-1960s, reaching 4.1–8.1 mg m^{-3} in the late-1970s. Annual GMs for the polyhaline salinity zone showed high interannual variability during the CBP Monitoring Program, ranging broadly from 4.0 to 11 mg m^{-3} and reaching current (2006–11) values of 5.4–7.2 mg m^{-3}.

Airborne remote sensing of ocean color (http://www.cbrsp.org) revealed strongly contrasting *chl-a* distributions in warm/wet and cool/dry years (Fig. 3a–c). Surface *chl-a* during the spring bloom ranged 10–20 mg m^{-3} in warm/wet years, compared to 4–8 mg m^{-3} in cool/dry years, with a LTA (16 years)~6–10 mg m^{-3}. This effect of climate variability on surface *chl-a* prompted us to incorporate the effects of freshwater flow in our statistical models, producing numerical *chl-a* criteria for low-flow, mid-flow, and high-flow conditions.

Mid-flow outputs of surface *chl-a* as GMs and 90th percentile thresholds for the 1960s and 1970 illustrate the spatial and temporal variability of numerical *chl-a* criteria (Fig. 4a, b). GMs for the 1960s and 1970s ranged 1.4–11 mg m^{-3} in spring and 1.6–17 mg m^{-3} in summer. Model outputs were lower for the 1960s than the 1970s for all three salinity zones in both spring and summer. GMs for the 1960s presented as goals ranged 1.4–5.9 mg m^{-3} in spring and 1.6–15 mg m^{-3} in summer, with the highest values for the oligohaline salinity zone and the lowest for the polyhaline salinity zone. The 90th percentile thresholds for the 1960s presented as

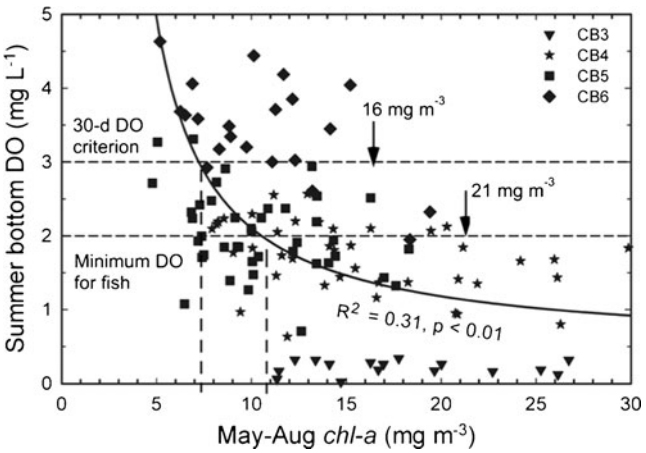

Fig. 5 Non-linear regression (negative, hyperbolic) of mean bottom-layer DO on mean May–Aug surface *chl-a* for four stations in the oligohaline (CB3), mesohaline (CB4, CB5), and polyhaline (CB6) salinity zones of the bay. *Vertical arrows* show surface *chl-a* corresponding to minimum DO criteria for fish (2 mg L^{-1}) and the 30-day DO criterion (3 mg L^{-1}). The 30-day mean DO criterion is based on deep-water DO concentrations that protect against losses in egg survival and larval recruitment of fish species inhabiting subpycnocline waters during summer months (US Environmental Protection Agency 2003). *Dashed vertical lines* show surface *chl-a* corresponding to intersections of the regression line with these DO criteria. The R^2 value and significance level of the regression are shown on the panel

compliance limits ranged 4.3–18 mg m^{-3} in spring and 5.0–45 mg m^{-3} in summer. GMs and 90th percentile thresholds for depth-averaged *chl-a* were similar to those for surface *chl-a* and are presented in Supplemental Material.

Model outputs as GMs and 90th percentile thresholds under low-flow, mid-flow, and high-flow conditions provide goals and compliance limits accounting for climate variability (Table 1). GMs for the mesohaline and polyhaline salinity zones were higher under high-flow than low-flow conditions, increasing from 2.2 to 3.3 mg m^{-3} for the mesohaline and from 1.1 to 2.2 mg m^{-3} for the polyhaline in spring, with similar responses to flow in summer. The effects of flow were opposite in sign for the oligohaline salinity zone with lower GMs under high-flow conditions. Flow conditions also affected the 90th percentile thresholds, with higher thresholds for mesohaline and polyhaline salinity zones under high-flow conditions than under mid- or low-flow conditions and higher thresholds for the oligohaline salinity zone under low-flow than under high-flow conditions.

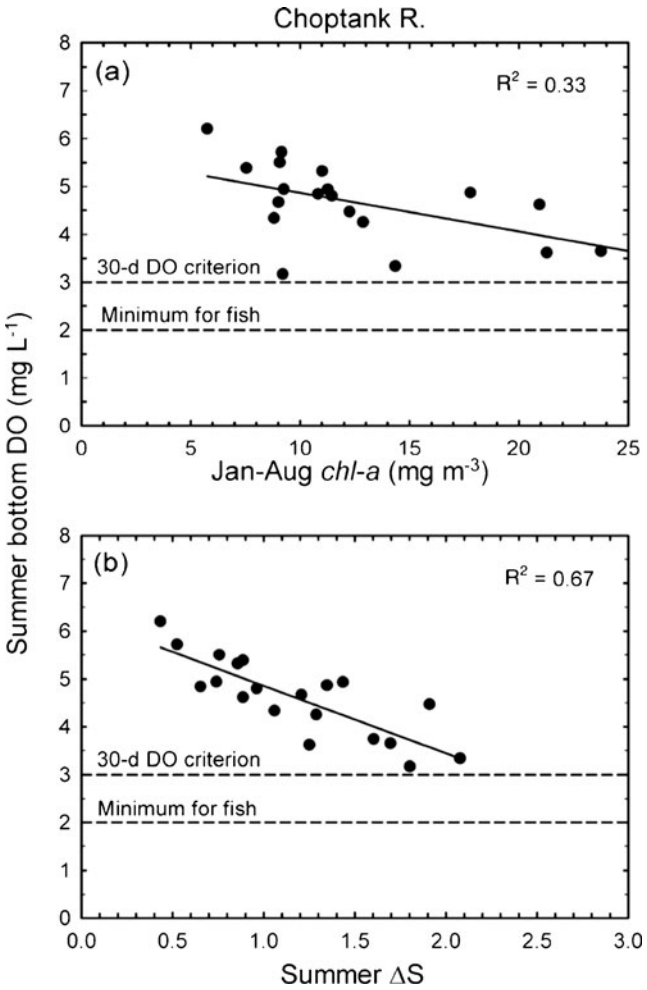

Fig. 6 Linear regressions of: **a** mean bottom-layer DO on mean Jan–Aug surface *chl-a*; **b** mean bottom-layer DO on summer ΔS for the tidal Choptank River

Dissolved Oxygen

Significant relationships were found between *chl-a*, depth, and DO using data for the mainstem bay. Simple linear regression of mean summer bottom-water DO on depth explained a significant ($p<0.05$) amount of the variance ($R^2=0.57$). Adding a term for *chl-a* (mean Jan–Aug *chl-a*) to depth produced a significant MLR model with an increased R^2:

$$\mathrm{DO} = 5.84 - 0.0519 \times chl\text{-}a - 0.0946 \times \mathrm{depth} \quad (R^2 = 0.63,\ p = 0.031) \tag{2}$$

A MLR model including terms for *chl-a*, depth, and ΔS had a greater R^2 than Eq. 2, but just exceeded the minimum value for significance ($p=0.057$).

We found significant negative relationships between mean summer bottom-water DO and mean surface *chl-a* for the bay and two tidal tributaries. Table 2 summarizes the statistics for simple linear regressions of bottom-water DO on surface *chl-a* averaged over several time scales (i.e., calendar year, water year, Jan–Aug, May–Aug). There was a significant, negative hyperbolic relationship between mean summer bottom-water DO and mean May–Aug *chl-a* using data for stations in the mainstem bay ($R^2=0.31$, $p<0.01$) that explained a greater amount of the variance than a linear fit (Fig. 5). A shift to low summer bottom-water DO occurred at high *chl-a*, with no observations of DO>3 mg L^{-1} at mean May–Aug *chl-a*>16 mg m^{-3} or DO>2.0 mg L^{-1} at mean May–Aug *chl-a*>21 mg m^{-3} (vertical arrows, Fig. 5).

Ecosystem impairments by low DO were defined by values of 3 and 2 mg L^{-1}. These are depicted as horizontal dashed lines on Fig. 5, representing the deep-water 30-day mean DO

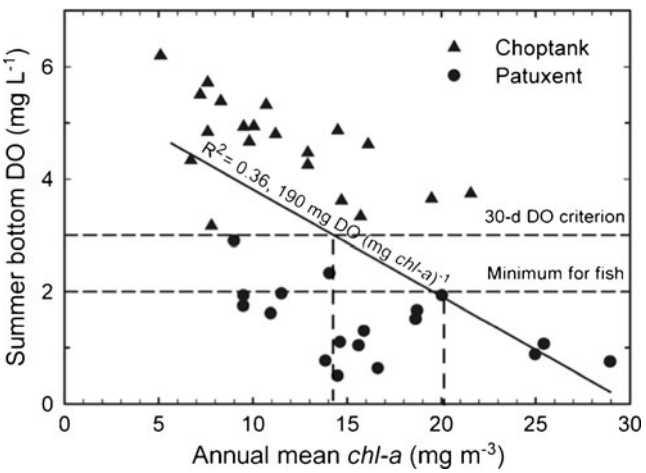

Fig. 7 Linear regression of bottom-layer DO in summer on annual mean surface *chl-a* for the Choptank and Patuxent Rivers. *Dashed vertical lines* show surface *chl-a* corresponding to intersections of the regression line with 2 and 3 mg L^{-1} DO criteria (see Fig. 6). The R^2 value and significance level of the regression are shown on the panel

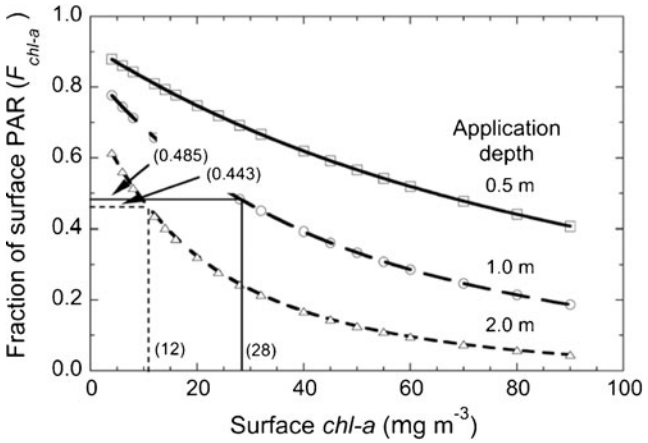

Fig. 8 Fraction of surface PAR ($F_{chl\text{-}a}$) remaining at three application depths as a function of surface *chl-a*, calculated using *Hydrolight* with a phytoplankton absorption spectrum for Chesapeake Bay and a case 1 bio-optical model for CDOM and scattering. *Dotted line* shows surface *chl-a* of 12 mg m^{-3} derived for a 2-m application depth and the allowable fraction for SAV in tidal-fresh and oligohaline salinity zones ($F_{chl\text{-}a}$=0.443); *solid line* shows surface *chl-a* of 28 mg m^{-3} derived for 1-m application depth ($F_{chl\text{-}a}$=0.485, see Table 4)

criterion and the minimum DO for fish, respectively (US Environmental Protection Agency 2003). Surface *chl-a* corresponding to intersections of the non-linear regression with DO values of 3 and 2 mg L^{-1} were 7.2 and 10.7 (rounded to 11) mg m^{-3}, depicted by vertical dashed lines in Fig. 5. We present these concentrations as numerical *chl-a* criteria analogous to mean surface *chl-a* derived for historical reference periods. The attainment of May–Aug *chl-a* in this range is required to achieve increases of DO to the specified values in the mainstem Bay. May–Aug *chl-a* of 16 and 21 mg m^{-3} are values of *chl-a* above which no DO observations meeting DO criteria were observed. These higher values of *chl-a* are analogous to the 90th percentile thresholds that we derived using data for historical reference periods. We found DO<3 mg L^{-1} occurred in the oligohaline salinity zone (CB3) at mean May–Aug *chl-a* of 11–16 mg m^{-3}, likely reflecting the proximity to nutrient sources, bathymetry, and density stratification. Similarly, DO<2 mg L^{-1} occurred in the mesohaline salinity zone (CB4, CB5) at mean May–Aug *chl-a* of 6–10 mg m^{-3}, indicating reductions of *chl-a* from current conditions (Fig. 2) would be required to meet DO criteria for the mainstem Bay.

A negative relationship between DO and surface *chl-a* was also found for the tidal Choptank River. A MLR model showed a significant negative linear relationship of bottom-water DO and the independent variables mean Jan–Aug *chl-a* and ΔS, dominated by ΔS as:

$$\mathrm{DO} = 6.51 - 0.0361 * \text{Jan–Aug } chl\text{–}a - 1.22 * \Delta S \quad (R^2 = 0.73,\ p < 0.05) \tag{3}$$

Mean Jan–Aug *chl-a*>15 mg m^{-3} was associated with bottom-water DO of 3–5 mg L^{-1}, and the lowest *chl-a* values were associated with the highest bottom-water DO (Fig. 6a). The relationship between DO and ΔS was stronger than between DO and surface *chl-a* (Fig. 6b). Substituting mean *chl-a* for different time frames as the biomass term in Eq. 3 produced similar relationships.

Comparative data for the tidal Choptank and Patuxent Rivers showed similar negative relationships of summer bottom-water DO and surface *chl-a*, using annual mean *chl-a* as the biomass term (Fig. 7). DO decreased with increased *chl-a* in the tidal Choptank River, but did not decline below 3 mg L^{-1}, even at annual mean *chl-a*>20 mg m^{-3}. DO was <2 mg L^{-1} in the tidal Patuxent River at annual mean *chl-a* of 9–11 mg m^{-3} and decreased further to ~1 mg L^{-1} at annual mean *chl-a*≥14 mg m^{-3}. Simple linear regression showed a significant (p<0.01) negative relationship between summer bottom-water DO and annual mean *chl-a* using data for these contrasting tributaries (Fig. 7). The slope of the regression represents a *chl-a*-specific decline of summer bottom-water

Table 3 *Chl-a* criteria derived from *Hydrolight* 4.2 modeling of light attenuation by *chl-a* and phytoplankton-derived CDOM

		Tidal fresh/oligohaline		Mesohaline/polyhaline	
		F_{lr}=0.13		F_{lr}=0.22	
SSAV application depth (m)	F_{Zw}	$F_{chl\text{-}a}$	*chl-a* (mg m^{-3})	$F_{chl\text{-}a}$	*chl-a* (mg m^{-3})
0.5	0.920	0.511	62	0.599	44
1.0[a]	0.853	0.485	28	0.568	19
2.0[b]	0.748	0.443	12	0.518	7.9

F_{lr} fraction of surface PAR required by SAV in different salinity zones, F_{Zw} fraction of surface PAR penetrating to a given SAV application depth accounting for attenuation by pure sea water alone, $F_{chl\text{-}a}$ fraction of surface PAR required to penetrate to three SAV application depths after allocating 30 % of non-water light attenuation to *chl-a* and phytoplankton-derived CDOM, *chl-a* concentration allowing the fraction, $F_{chl\text{-}a}$, of surface PAR to penetrate to a given application depth

[a] 1.0 m application depth is the Tier 2 SAV restoration goal established by EPA (Batiuk et al. 1992)

[b] 2.0 m application depth is the Tier 3 SAV restoration goal

DO of 190 mg O_2 (mg *chl-a*)$^{-1}$. Vertical dashed lines in Fig. 7 show intersections of the regression line with DO criteria of 3 and 2 mg L^{-1}, corresponding to annual mean *chl-a* of 14.2 mg m^{-3} as the numerical *chl-a* criterion and a threshold of 20.1 mg m^{-3} (rounded to 14 and 20 mg m^{-3}). These relatively high values reflect the different DO–*chl-a* relationships in the tidal Choptank and Patuxent Rivers. Annual mean *chl-a*>20 mg m^{-3} would meet DO criteria in the Choptank River, while *chl-a*<9 mg m^{-3} would be required to achieve DO>2–3 mg L^{-1} in the Patuxent River (Fig. 7).

Water Clarity

Radiative transfer modeling with *Hydrolight* demonstrated that the fraction of surface PAR reaching three SAV application depths declined monotonically with *chl-a* due to light attenuation by *chl-a* and phytoplankton-derived CDOM (Fig. 8). Procedures for calculating mean and threshold *chl-a* concentrations are illustrated for a 2-m application depth and a light requirement of 13 % (F_{lr}=0.13) applicable to SAV in tidal fresh and oligohaline salinity zones. For the fraction transmitted to 2 m by pure water, F_{Zw}=0.748, we calculated the fraction of surface irradiance that must remain after attenuation by *chl-a*, $F_{chl\text{-}a}$=0.443, using Eq. 1. Mean surface *chl-a* permitting 0.443 of surface PAR to reach an application depth of 2 m was then computed as 12 mg m^{-3} (Table 3; Fig. 8). Following the same procedures, using the fraction transmitted to 1 m by pure water, F_{Zw}=0.853, we calculated the fraction of surface irradiance that must remain at the shallower application depth after attenuation by *chl-a*, $F_{chl\text{-}a}$=0.485. Mean surface *chl-a* permitting 0.485 of surface PAR to reach an application depth of 1 m was then computed as 28 mg m^{-3} (Table 3; Fig. 8).

Model outputs for application depths of 2 and 1 m in the tidal-fresh and oligohaline salinity zones illustrate surface *chl-a* that allow sufficient light penetration to meet SAV restoration targets (Fig. 8). Surface *chl-a* concentrations permitting SAV restoration to 2 and 1 m, respectively, are analogous to the means and thresholds for *chl-a* based on historical analyses and other ecosystem impairments proposed as numerical *chl-a* criteria. Applied to other application depths and light requirements, $F_{chl\text{-}a}$ ranged from 0.443 to 0.511 for the tidal fresh and oligohaline salinity zones where SAV require 13 % of surface PAR (Kemp et al. 2004) and from 0.518 to 0.599 for mesohaline and polyhaline zones where SAV require 22 % of surface PAR (Table 3). These values correspond to surface *chl-a* of 12–62 mg m^{-3} for tidal fresh and oligohaline salinity zones and 7.9–44 mg m^{-3} for mesohaline and polyhaline salinity zones (Table 3; Fig. 9). Mean surface *chl-a* for application depths

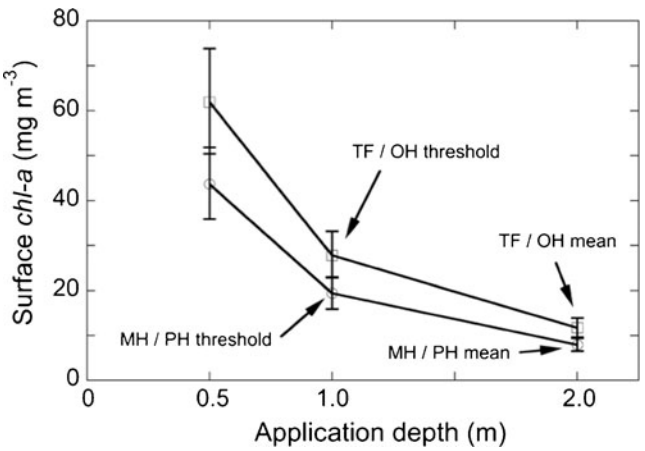

Fig. 9 *Hydrolight* derivations of numerical *chl-a* criteria as a function of application depth for SAV having light requirements characteristic of tidal-fresh and oligohaline (TF/OH) salinity zones (*squares*), and mesohaline and polyhaline (MH/PH) salinity zones (*circles*). *Vertical bars* show the range of variation in *chl-a* criteria calculated by varying the fraction of non-water attenuation allocated to *chl-a* from 0.25 (*lower bar*) to 0.35 (*upper bar*)

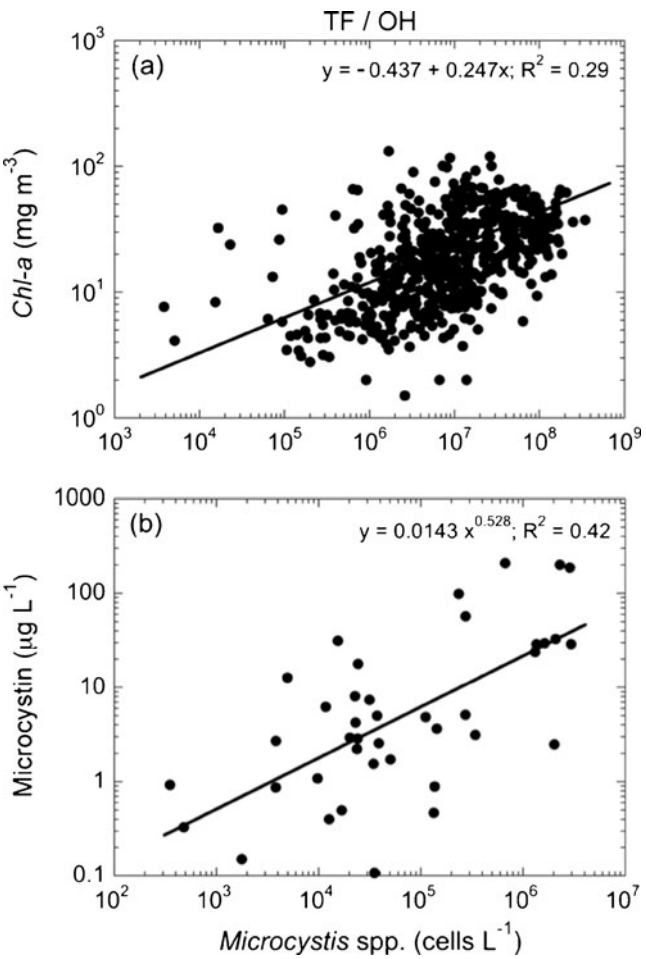

Fig. 10 Simple, linear regressions of: **a** *Microcystis* spp. abundance (in cells per liter) on *chl-a* (in milligrams per cubic meter) (log–log) for tidal-fresh and oligohaline (TF/OH) salinity zones; **b** concentrations of the toxin microcystin on cell counts of *Microcystis* spp

of 2 and 1 m as goals and compliance limits, respectively, were 7.9 and 19 mg m^{-3} for mesohaline and polyhaline salinity zones and 12 and 28 mg m^{-3} for tidal fresh and oligohaline salinity zones. Varying the fraction of attenuation allocated to *chl-a* and phytoplankton-derived CDOM from 0.25 to 0.35 at each application depth and salinity zone produced ~18 % variation around the value obtained using 0.30 as the fraction, depicted as range bars in Fig. 9.

Toxic Algal Blooms

Concurrent measurements of surface *chl-a* and cell counts of *Microcystis* spp. in tidal fresh and oligohaline salinity zones experiencing toxic blooms (salinity≤5) showed a significant log-linear relationship ($p<0.05$) for upper Chesapeake Bay and four of seven tidal tributaries (Fig. 10a), with the strongest relationship observed for the Potomac River (Table 4). A positive log-linear relationship ($p<0.05$) was also found between cell counts of *Microcystis* spp. and microcystin concentrations (Fig. 10b), enabling us to link toxin concentrations to surface *chl-a*. CART analysis indicated a *chl-a* threshold separating high-level risk of exposure to microcystin from middle- and low-level risk of 29 mg m^{-3}. We considered published management-action *chl-a* from Australian studies (NHMRC 2005) and results of CART analysis to establish a *chl-a* threshold of 28 mg m^{-3} that would be protective against toxic *Microcystis* spp. in the tidal fresh and oligohaline salinity zones of Chesapeake Bay (US Environmental Protection Agency 2007a, b). This value was lowered further to 25 mg m^{-3} based on cumulative impacts of microcystin exposure, synergistic effects of toxins (anatoxin-a and microcystin), and the co-occurrence of multiple toxins during blooms (Fitzgeorge et al. 1994; Tango and Butler 2008). Mean *chl-a* of 15 mg m^{-3} corresponding to the 90th percentile threshold of 25 mg m^{-3} was computed using the frequency distribution of surface *chl-a* data from the CBP Monitoring Program for waters impacted by *Microcystis* spp. blooms.

Table 4 Regression statistics (log–log) for *Microcystis* (in cells per liter) on *chl-a* (in milligrams per cubic meter) for upper Chesapeake Bay and tidal tributaries (1984–2004)

Subestuary	*n*	Regression equation	R^2	*p* value
Upper Bay	102	$y=0.186x-0.285$	0.20	<0.0001
Choptank R.	95	$y=0.138x+0.192$	0.24	<0.0001
Patapsco R.	7	$y=0.211x-1.133$	0.27	0.235
Patuxent R.	107	$y=0.230x-0.044$	0.19	<0.0001
Potomac R.	148	$y=0.304x-0.913$	0.54	<0.0001
James R.	85	$y=0.125x+0.520$	0.09	0.0143
Rappahannock R.	44	$y=0.072x+0.731$	0.04	0.231
York R.	27	$y=0.080x+0.362$	0.06	0.280

Discussion

Setting numerical water quality criteria has important implications for managing water quality and sustaining living resources in coastal ecosystems. Our approach addressed these requirements by combining retrospective assessments of water quality conditions prior to declines in the spatial extent of SAV and increases in DO-depleted bottom waters with process-based analyses to establish site-specific links between water quality concentrations (*chl-a*) and impairments. We

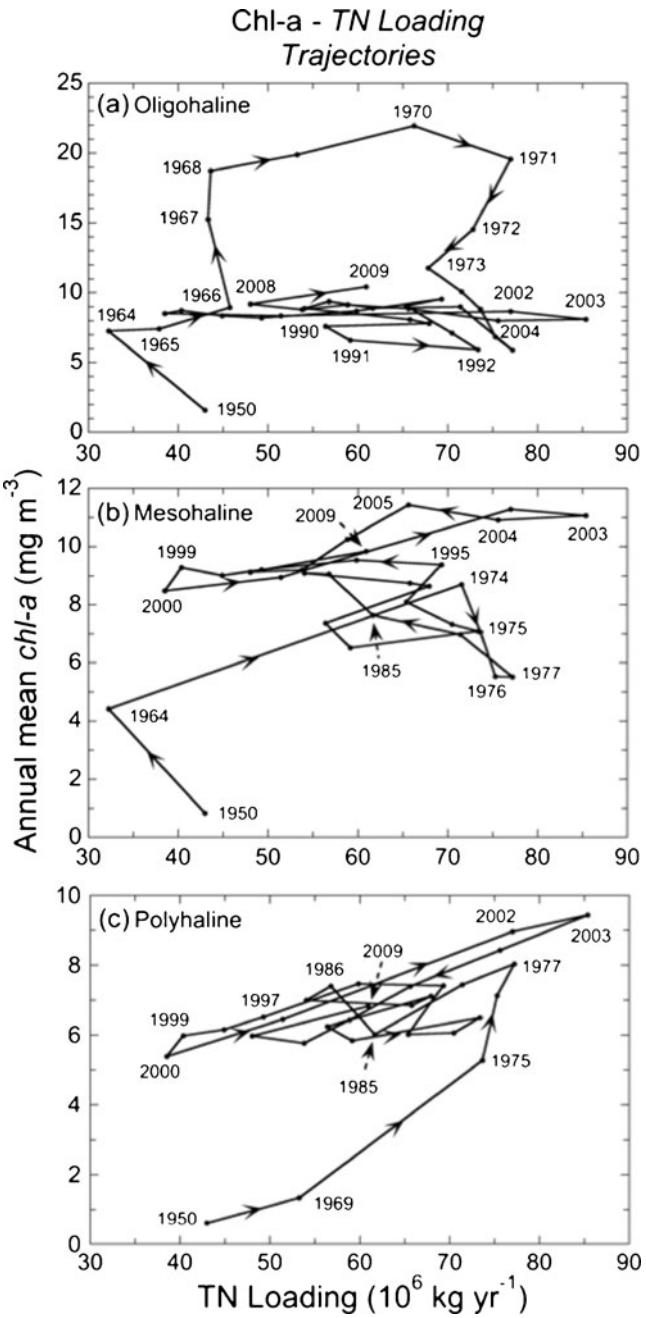

Fig. 11 **a–c** Historical trajectories of annual mean *chl-a* vs. TN loading for oligohaline, mesohaline, and polyhaline salinity zones

suggest this approach is relevant to ongoing efforts at setting criteria for other coastal ecosystems, although the water quality parameters and specific impairments may differ. Details on derivation and implementation, attainability, and linkage to impairments are discussed below.

Derivation and Implementation

Baseline *chl-a* data were not available for Chesapeake Bay prior to European settlement or for the next three centuries, complicating an assessment of anthropogenic influences on the ecosystem. Measurements in the post-World War II period (1950s–1970s) provided the earliest data for a less-impacted bay, supporting development of numerical *chl-a* criteria based on historical reference periods (Table 1). A similar statistical approach was proposed recently for Florida coastal waters using SeaWiFS satellite retrievals of *chl-a* (1997–2010) combined with in situ observations (Schaeffer et al. 2012). We derived numerical *chl-a* criteria using statistical models for two periods (1960s and 1970s), two seasons (spring and summer), three salinity zones (oligohaline, mesohaline, and polyhaline), and three flow conditions (low, mid, and high flow). The resulting GMs and 90th percentile thresholds constitute goals and compliance limits, respectively (Fig. 4a, b; Table 1). Here we propose implementation of criteria based on the 1960s historical reference period, including flow adjustments to account for climate variability.

Attainability

Adhering to numerical *chl-a* criteria presented here (Table 1) will require sustained reductions in nutrient loading which begs the question, are numerical *chl-a* criteria based on historical reference periods attainable? Duarte et al. (2009) presented the concept of "Neverland" for several northern European ecosystems, arguing from *chl-a* vs. TN loading trajectories that a return to less-impacted conditions by reducing nutrients may take a non-linear route so that reaching pre-enrichment *chl-a* levels may be unrealistic. Carstensen et al. (2011) applied a similar approach using annual average *chl-a* vs. nutrient concentrations for a range of coastal ecosystems to emphasize the need to consider shifting baselines. Multiple changes in these ecosystems during the eutrophication period when nutrient inputs increased dramatically were reasoned to make a straight-line decline to lower *chl-a* with nutrient reductions alone an improbable trajectory. Given changes in the impacts of human expansion on Chesapeake Bay, such as increases in N loading, habitat loss, and overfishing (Rothschild et al. 1994; Boynton et al. 1995; Hagy et al. 2004; Kemp et al. 2005; Lellis-Dibble et al. 2008), shifting baselines is likely to be an issue for Chesapeake Bay as well. An optimistic sign for Chesapeake Bay is that the regression slopes of annual average *chl-a* vs. TN concentrations for the mesohaline and polyhaline salinity zones were among the steepest for 28 study areas (Carstensen et al. 2011; their Fig. 3), suggesting responsiveness to nutrient reductions.

Pursuing the reasoning of Duarte et al. (2009), our analysis of *chl-a* vs. TN loading trajectories using data for Chesapeake Bay aggregated by salinity zone revealed non-linearities comparable to other systems, particularly for the oligohaline salinity zone (Fig. 11a–c). Annual mean *chl-a* during the 1970s was >20 mg m^{-3} in the oligohaline salinity zone and declined to half that concentration following the phosphate ban (Fisher et al. 1992) in the early to mid-1980s (Fig. 11a). This decrease of *chl-a* in the oligohaline salinity zone was apparently a result of increased P-limitation after the mid-1980s (Fisher et al. 1992, 1999). This led to present-day concentrations ~8–12 mg m^{-3} at similar TN loadings as occurred in the past (Fig. 2a). These findings suggest that N-limitation was more pronounced in the mesohaline and polyhaline salinity zones during the 1950s–1970s, contributing to lower *chl-a* in seaward regions of the bay. We believe that phytoplankton intercepted more N and P when they attained higher biomass in the once P-replete oligohaline salinity zone, leading to decreased throughput of N to the mesohaline and polyhaline

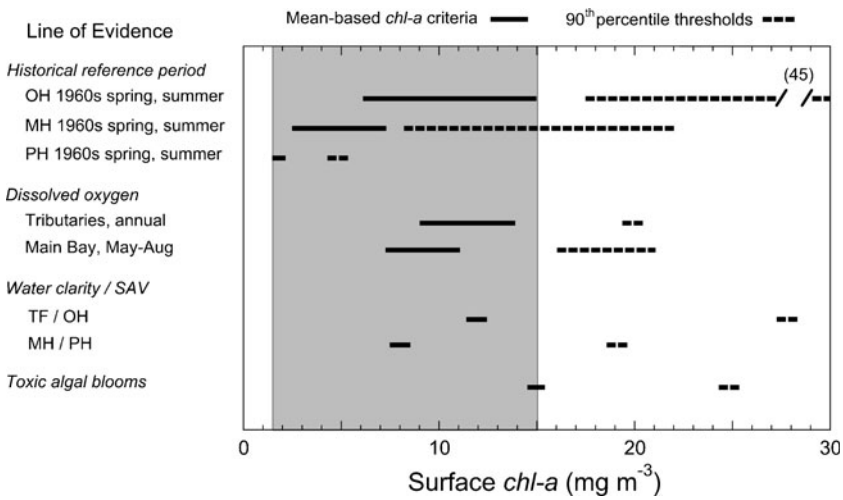

Fig. 12 Graphic comparison of numerical *chl-a* criteria developed using multiple lines of evidence, showing means as goals (*solid lines*) and 90th percentile thresholds as compliance limits (*dashed lines*). The 90th percentile of log-normal distributions of *chl-a* was used directly to establish thresholds for historical reference periods and toxic algal blooms, and the analogous approach for DO and water clarity/SAV used specific target values for *chl-a* related to these ecosystem impairments

salinity zones (cf. Paerl et al. 2004) where N-limitation prevails (Malone et al. 1996).

Climate variability during the last three decades has generated large interannual differences of freshwater flow and nutrient loading. High-flow conditions delivered more nutrients resulting in higher *chl-a* (Fig. 3a) while low-flow conditions led to increased nutrient limitation and lower *chl-a* (Fig. 3c). Shipboard, aircraft, and satellite observations documented the effects of climate variability on seasonal to interannual variability of phytoplankton biomass, floral composition, and primary productivity (cf. Acker et al. 2005; Adolf et al. 2006; Miller and Harding 2007). Numerical *chl-a* criteria consisting of GMs and 90th percentile thresholds for low-flow, mid-flow, and high-flow conditions (Table 1) provide goals and compliance limits adjusted for climate variability (Fig. 3). Aligning these values with actual freshwater flow for a given year constitutes implementation of flow-specific numerical *chl-a* criteria, allowing us to gauge progress while taking account of climate variability. This is an important step to separate short-term effects on *chl-a* traceable to climate variability from long-term trends that signal oligotrophication.

Linkage to Impairments

Relationships of *chl-a* to DO, water clarity, and toxic algae were used to develop numerical *chl-a* criteria based on ecosystem impairments, producing goals and compliance limits comparable to those for historical reference periods (Table 1; Fig. 12). Relationships between *chl-a* and DO indicate mean May–Aug *chl-a* of 7.2–11 mg m^{-3} in the deeper Bay (Fig. 5), and annual mean *chl-a* of 9.0–14 mg m^{-3} in the tidal tributaries (Fig. 7) would preclude low DO. Radiative transfer modeling using *Hydrolight* showed that sufficient light conditions for SAV would require mean *chl-a* of 7.9–12 mg m^{-3} with thresholds of 19–28 mg m^{-3} during the growing seasons for 2- and 1-m application depths, respectively (Table 3; Fig. 9). Cell counts of *Microcystis aeruginosa* linked to *chl-a* and microcystin concentrations supported a goal of 15 mg m^{-3} and a threshold of 25 mg m^{-3} for mean summer *chl-a* (Table 4; Fig. 10a, b) that would lower the risk of human-health effects due to toxic cyanobacteria (US Environmental Protection Agency 2007a, b, 2008). These ranges of numerical *chl-a* criteria are consistent for several ecosystem impairments (Fig. 12), despite the different spatial and temporal domains they cover. This congruence is encouraging and further supports our suggestion that the general approach adopted here should have wide applicability in other systems.

Recognizing that major reductions of nutrient loading will be required to adhere to goals and compliance limits for *chl-a* based on the 1960s historical reference period, we suggest that the adoption, application, and enforcement of these criteria will move the bay toward conditions when ecosystem impairments were less severe. Certainly, coastal ecosystems such as Chesapeake Bay have changed in many ways in addition to nutrient loading, but implementation of numerical *chl-a* criteria based on conditions in a less-impacted ecosystem, supported by scientific evidence on impairments linked to *chl-a*, is a prudent approach that we believe will have positive consequences.

Acknowledgments LWH was supported by the NSF Biological Oceanography Program and the NOAA Chesapeake Bay Program Office. TRF was supported by the NASA Land-Use Land-Cover Change Program and the NSF Ecosystems Science Programs. MRM was supported by the NSF Ecological and Evolutionary Physiology Program and the Virginia Environmental Endowment. HWP was supported by the NSF Biological Oceanography Program and the North Carolina Department of Environment and Natural Resources, ModMon and FerryMon Projects.

References

Acker, J.G., L.W. Harding, G. Leptoukh, T. Zhu, and S. Shen. 2005. Remotely-sensed chl *a* at the Chesapeake Bay mouth is correlated with annual freshwater flow to Chesapeake Bay. *Geophysical Research Letters* 32: L05601. doi:10.1029/2004GL021852.

Adolf, J.E., C.L. Yeager, W.D. Miller, M.E. Mallonee, and L.W. Harding Jr. 2006. Environmental forcing of phytoplankton floral composition, biomass, and primary productivity in Chesapeake Bay, *USA. Estuarine, Coastal and Shelf Science* 67: 108–122.

Batiuk, R.A., R.J. Orth, K.A. Moore, W.C. Dennison, J.C. Stevenson, L.W. Staver, V. Carter, N. Rybicki, R.E. Hickman, S. Kollar, S. Bieber and P. Heasly. 1992. Chesapeake Bay submerged aquatic vegetation habitat requirements and restoration targets: a technical synthesis. USEPA-CBP 68-WO-0043. Annapolis: US Environmental Protection Agency.

Boynton, W.R., J.H. Garber, R. Summers, and W.M. Kemp. 1995. Inputs, transformations, and transport of nitrogen and phosphorus in Chesapeake Bay and selected tributaries. *Estuaries* 18: 285–314.

Bricker, S., B. Longstaff, W. Dennison, A. Jones, K. Boicourt, C. Wicks and J. Woerner. 2007. Effects of nutrient enrichment in the Nation's estuaries: a decade of change. NOAA Coastal Ocean Program Decision Analysis Series No. 26. Silver Spring: National Centers for Coastal Ocean Science. 328 p.

Carstensen, J., M. Sanchez-Camacho, C.M. Duarte, D. Krause-Jensen, and N. Marba. 2011. Connecting the dots: responses of coastal ecosystems to changing nutrient concentrations. *Environmental Science and Technology* 45: 9122–9132.

Carter, V., N.B. Rybicki, J.M. Landwehr, and M. Naylor. 2000. Light requirements for SAV survival and growth. In *Chesapeake Bay submerged aquatic vegetation water quality and habitat-based requirements and restoration targets: a second technical synthesis*, ed. R.A. Batiuk, P. Bergstrom, W.M. Kemp, E.W. Koch, L. Murray, J.C. Stevenson, R. Bartleson, V. Carter, N.B. Rybicki, J.M. Landwehr, C.L. Gallegos, L. Karrh, M. Naylor, D.J. Wilcox, K.A. Moore, S. Ailstock, and M. Teichberg, 4–15. Annapolis: US Environmental Protection Agency, Chesapeake Bay Program.

Chorus, I. and J. Bartram. (Eds.) 1999. *Toxic cyanobacteria in water: a guide to their public health consequences, monitoring and management.* London: World Health Organization.

Dennison, W.C., R.J. Orth, K.A. Moore, J.C. Stevenson, V. Carter, S. Kollar, P. Bergstrom, and R. Batiuk. 1993. Assessing water quality

with submersed aquatic vegetation. Habitat requirements as barometers of Chesapeake Bay health. *Bioscience* 43: 86–94.

Duarte, C.M., D.J. Conley, J. Carstensen, and M. Sanchez-Camacho. 2009. Return to *Neverland*: shifting baselines affect eutrophication restoration targets. *Estuaries and Coasts* 32: 29–36.

Fisher, T.R., A.B. Gustafson\, K. Sellner, R. Lacouture, L.W. Haas, R. Magnien, R. Karrh, and B. Michael. 1999. Spatial and temporal variation in resource limitation in Chesapeake Bay. *Marine Biology* 133: 763–778.

Fisher, T.R., J.D. Hagy III, W.R. Boynton, and M.R. Williams. 2006. Cultural eutrophication in the Choptank and Patuxent estuaries of Chesapeake Bay. *Limnology and Oceanography* 51: 435–447.

Fisher, T.R., L.W. Harding Jr., D.W. Stanley, and L.G. Ward. 1988. Phytoplankton, nutrients, and turbidity in the Chesapeake, Delaware, and Hudson estuaries. *Estuarine, Coastal and Shelf Science* 27: 61–93.

Fisher, T.R., E.R. Peele, J.W. Ammerman, and L.W. Harding Jr. 1992. Nutrient limitation of phytoplankton in Chesapeake Bay. *Marine Ecology Progress Series* 82: 51–63.

Fitzgeorge, R.B., S.A. Clark, and C.W. Kevil. 1994. Routes of intoxication. In *Detection methods for cyanobacterial toxins*, ed. G.A. Codd, T.M. Jeffries, C.W. Keevil, and E. Potter, 69–74. Cambridge: The Royal Society of Chemistry.

Gallegos, C.L. 1994. Refining habitat requirements of submersed aquatic vegetation: role of optical models. *Estuaries* 17: 198–219.

Gallegos, C.L. 2001. Calculating optical water quality targets to restore and protect submersed aquatic vegetation: overcoming problems in partitioning the diffuse attenuation coefficient for photosynthetically active radiation. *Estuaries* 24: 381–397.

Hagy III, J.D., W.R. Boynton, C.W. Wood, and K.V. Wood. 2004. Hypoxia in Chesapeake Bay, 1950–2001: long-term change in relation to nutrient loading and river flow. *Estuaries and Coasts* 27: 634–658.

Harding Jr., L.W., and E.S. Perry. 1997. Long-term increase of phytoplankton biomass in Chesapeake Bay, 1950–1994. *Marine Ecology Progress Series* 157: 39–52.

Harding Jr., L.W., A. Magnuson, and M.E. Mallonee. 2005. SeaWiFS retrievals of chlorophyll in Chesapeake Bay and the mid-Atlantic bight. *Estuarine, Coastal and Shelf Science* 62: 75–94.

Harding Jr., L.W., B.W. Meeson, and T.R. Fisher Jr. 1986. Phytoplankton production in two east coast estuaries: photosynthesis-light functions and patterns of carbon assimilation in Chesapeake and Delaware Bays. *Estuarine, Coastal and Shelf Science* 23: 773–806.

Kemp, W.M., R. Batiuk, R. Bartleson, P. Bergstrom, V. Carter, G. Gallegos, W. Hunley, L. Karrh, E. Koch, J. Landwehr, K. Moore, L. Murray, M. Naylor, N. Rybicki, J.C. Stevenson, and D. Wilcox. 2004. Habitat requirements for submerged aquatic vegetation in Chesapeake Bay: water quality, light regime, and physical-chemical factors. *Estuaries* 27: 263–377.

Kemp, W.M., W.R. Boynton, J.E. Adolf, D.F. Boesch, W.C. Boicourt, G. Brush, J.C. Cornwell, T.R. Fisher, P.M. Glibert, J.D. Hagy, L.W. Harding Jr., E.D. Houde, D.G. Kimmel, W.D. Miller, R.I.E. Newell, M.R. Roman, R.M. Smith, and J.C. Stevenson. 2005. Eutrophication of Chesapeake Bay: historical trends and ecological interactions. *Marine Ecology Progress Series* 303: 1–29.

Kirk, J.T.O., R.W. Spinrad, K.L. Carder, and M.J. Perry. 1994. The relationship between the inherent and the apparent optical properties of surface waters and its dependence on the shape of the volume scattering function. In *Ocean optics*, 40–58. Oxford: Oxford Monographs on Geology and Geophysics, Oxford University Press.

Lellis-Dibble, K.A., K.E. McGlynn and T.E. Bigford. 2008. U.S. commercial and recreational fisheries: economic value as an incentive to protect and restore estuarine habitat. NOAA Technical Memorandum NMFS-F/SPO-90

Magnuson, A., L.W. Harding Jr., M.E. Mallonee, and J.E. Adolf. 2004. Bio-optical model for Chesapeake Bay and the Middle Atlantic Bight. *Estuarine, Coastal and Shelf Science* 61: 403–424.

Malone, T.C. 1992. Effects of water column processes on dissolved oxygen: nutrients, phytoplankton and zooplankton. In *Oxygen dynamics in Chesapeake Bay: a synthesis of research*, ed. D. Smith, M. Leffler, and G. Mackiernan, 61–112. College Park: University of Maryland Sea Grant.

Malone, T.C., D.J. Conley, T.R. Fisher, P.M. Glibert, and L.W. Harding Jr. 1996. Scales of nutrient limited phytoplankton productivity in Chesapeake Bay. *Estuaries* 19: 371–385.

Malone, T.C., L.H. Crocker, S.E. Pike, and B.W. Wendler. 1988. Influences of river flow on the dynamics of phytoplankton production in a partially stratified estuary. *Marine Ecology Progress Series* 48: 235–249.

Marshall, H.G., L. Burchardt, and R. Lacouture. 2005. A review of phytoplankton composition within Chesapeake Bay and its tidal estuaries. *Journal of Plankton Research* 27: 1083–1102.

Marshall, H.G., M.F. Lane, K.K. Nesius, and L. Burchardt. 2009. Assessment and significance of phytoplankton species composition within Chesapeake Bay and Virginia tributaries through a long-term monitoring program. *Environmental Monitoring and Assessment* 150: 143–155.

Miller, W.D., and L.W. Harding Jr. 2007. Climate forcing of the spring bloom in Chesapeake Bay. *Marine Ecology Progress Series* 331: 11–22.

Miller, W.D., D.G. Kimmel, and L.W. Harding Jr. 2006. Predicting spring discharge of the Susquehanna River from a winter synoptic climatology for the eastern United States. *Water Resources Research* 42: W05414. doi:10.1029/2005WR004270.

Mobley, C.D. 1994. *Light and water. Radiative transfer in natural waters*. San Diego: Academic.

Morse, R.E., J. Shen, J.L. Blanco-Garcia, W.S. Hunley, S. Fentress, M. Wiggins, and M.R. Mulholland. 2011. Environmental and physical controls on the formation and transport of blooms of the dinoflagellate *Cochlodinium polykrikoides* Margalef in lower Chesapeake Bay and its tributaries. *Estuaries and Coasts* 34: 1006–1025.

Mulholland, M.R., R.E. Morse, G.E. Boneillo, P.W. Bernhardt, K.C. Filippino, L.A. Procise, J.L. Blanco-Garcia, H.G. Marshall, T.A. Egerton, W.S. Hunley, K.A. Moore, D.L. Berry, and C.J. Gobler. 2009. Understanding causes and impacts of the dinoflagellate, *Cochlodinium polykrikoides*, blooms in the Chesapeake Bay. *Estuaries and Coasts* 32: 734–747.

NHMRC. 2005. *Guidelines for managing risk in recreational waters*. Canberra: Australian government National Health and Medical Research Council. 207 p.

Paerl, H.W., L.M. Valdes, M.F. Piehler, and M.E. Lebo. 2004. Solving problems resulting from solutions: the evolution of a dual nutrient management strategy for the eutrophying Neuse River Estuary, North Carolina. *Environmental Science and Technology* 38: 3068–3073.

Roesler, C.S., M.J. Perry, and K.L. Carder. 1989. Modeling *in situ* phytoplankton absorption from total absorption spectra in productive inland marine waters. *Limnology and Oceanography* 34: 1510–1523.

Rothschild, B.J., J.S. Ault, P. Goulletquer, and M. Heral. 1994. Decline of the Chesapeake Bay oyster population: a century of habitat destruction and overfishing. *Marine Ecology Progress Series* 111: 29–39.

SAS Institute, Inc. 1993. *SAS/ETS user's guide, version 6*, 2nd ed. Cary: SAS Institute.

S-Plus 7.0.6 for Windows. 2005. Seattle: Insightful Corporation.

Schaeffer, B.A., J.D. Hagy, R.N. Conmy, J.C. Lehrter, and R.P. Stumpf. 2012. An approach to developing numeric water quality criteria for coastal waters using the SeaWiFS satellite data record. *Environmental Science and Technology* 46: 916–922.

Schofield, O., T. Bergmann, M.J. Oliver, A. Irwin, G. Kirkpatrick, W.P. Bissett, M.A. Moline and C. Orrico. 2004. Inversion of spectral

absorption in the optically complex coastal waters of the Mid-Atlantic Bight. *Journal of Geophysical Research* 109: C12S04, 11–12. doi:10.1029/2003JC002071.

Smith, D.E., M. Leffler, and G. Mackiernan (eds.). 1992. *Oxygen dynamics in Chesapeake Bay: a synthesis of research*. College Park: University of Maryland Sea Grant. 234 p.

Tango, P., and W. Butler. 2008. Cyanotoxins in tidal waters of Chesapeake Bay. *Northeastern Naturalist* 15: 403–416.

US Environmental Protection Agency. 2003. *Ambient water quality criteria for dissolved oxygen, water clarity and chlorophyll a for Chesapeake Bay and its tidal tributaries.* EPA 903-R-03-002. Annapolis: US Environmental Protection Agency, Region 3, Chesapeake Bay Program Office.

US Environmental Protection Agency. 2007a. *Ambient water quality criteria for dissolved oxygen, water clarity and chlorophyll a for the Chesapeake Bay and its tidal tributaries. 2007 addendum*. EPA 903-R-07-003 CBP/TRS 285/07. Annapolis: US Environmental Protection Agency, Region 3 Chesapeake Bay Program Office.

US Environmental Protection Agency. 2007b. *Ambient water quality criteria for dissolved oxygen, water clarity and chlorophyll a for the Chesapeake Bay and its tidal tributaries. 2007 chlorophyll criteria addendum*. EPA 903-R-07-005 CBP/TRS 288/07. Annapolis: US Environmental Protection Agency, Region 3 Chesapeake Bay Program Office.

US Environmental Protection Agency. 2008. *Ambient water quality criteria for dissolved oxygen, water clarity and chlorophyll a for the Chesapeake Bay and its tidal tributaries. 2008 Technical support for criteria assessment protocols addendum.* EPA 903-R-08-001 CBP/TRS 290/08. Annapolis: US Environmental Protection Agency, Region 3 Chesapeake Bay Program Office.

Wood, S.N. 2006. *Generalized additive models (an introduction with R)*. Boca Raton: Chapman & Hall/CRC. 392 p.